# Kinetic and Mass Spectrometric Analyses of the Interactions between Plant Acetohydroxy Acid Isomeroreductase and Thiadiazole Derivatives†

Frédéric Halgand,‡,@ Françoise Vives,§,@ Renaud Dumas,*,§ Valérie Biou,|| Jens Andersen,‡ Jean-Pierre Andrieu,⊥ Richard Cantegril,# Jean Gagnon,⊥ Roland Douce,§ Eric Forest,‡ and Dominique Job§

*Laboratoire Mixte CNRS/Rhône-Poulenc (UMR 41) and Laboratoire de Synthèse Organique, Rhône-Poulenc Agrochimie, 14-20 rue Pierre Baizet, 69263 Lyon Cedex 9, France, and Laboratoire de Spectrométrie de Masse des Protéines, Laboratoire de Cristallographie Macromoléculaire, and Laboratoire d'Enzymologie Moléculaire, Institut de Biologie Structurale Jean-Pierre Ebel, 41 avenue des Martyrs, 38027 Grenoble Cedex 1, France*

*Received August 27, 1997; Revised Manuscript Received December 1, 1997*

ABSTRACT: Plant acetohydroxy acid isomeroreductase (EC 1.1.1.86), the second enzyme of the branched chain amino acid biosynthetic pathway, has been submitted to high-throughput screening for herbicide discovery. We report here the discovery of a new class of compounds belonging to the thiadiazole family, which exhibit a strong inhibitory effect on this plant enzyme. Kinetic analyses revealed that these compounds act as either reversible or irreversible noncompetitive inhibitors of the plant enzyme. Reversibility or irreversibility of these compounds can be attributed to the nature of the additional groups of the thiadiazole ring favoring or not favoring the formation of a covalent adduct. Mass spectrometric experiments on the complex between an irreversible compound belonging to the thiadiazole family and the plant enzyme identified Cys498 as the binding site of the inhibitor.

The branched chain amino acid metabolic pathway in plants is currently the object of intense study for the development of new classes of herbicides. For example, acetohydroxy acid synthase (acetolactate synthase, EC 4.1.3.18), which catalyzes the first common step in the parallel pathway leading to the biosynthesis of isoleucine, leucine, and valine, is the target of imidazolinones (*1*) and sulfonylureas (*2*). These compounds are among the most advanced herbicides used in agriculture because they exhibit extremely low mammalian toxicity and high efficacy, resulting in very low application rates and low environmental impact. However, because resistant plants can rapidly emerge under the selection pressure of these herbicides (*3*), it is important to evaluate the potentiality of other enzymes in the pathway to provide new efficient herbicide targets. Toward this goal, acetohydroxy acid isomeroreductase (EC 1.1.1.86), which is the second common enzyme of the parallel branched chain amino acid pathway, has been the subject of several studies, in both bacteria and plants. The enzyme catalyzes a $Mg^{2+}$-dependent two-step reaction (*4*) in which the substrate, either 2-acetolactate or 2-aceto-2-hydroxybutyrate (AHB[1]), is converted via an alkyl migration and a NADPH-dependent reduction to yield 2,3-dihydroxy-3-isovalerate (synthesis of valine and leucine) or 2,3-dihydroxy-3-methylvalerate (synthesis of isoleucine), respectively. The plant enzyme has been purified from spinach chloroplasts (*5*), and its cDNA has been cloned (*6*), allowing overproduction of the spinach chloroplast enzyme in *Escherichia coli* (*7*) and investigation of some of its kinetic and structural properties (*8*−*12*). The plant enzyme exists in solution as a homodimer of identical subunits with a $M_r$ of 57 000 and possesses two active site-located magnesium ions, one of which plays a role in the isomerization step and the other in the reduction step (*8*, *12*).

Transition state analogues such as *N*-hydroxy-*N*-isopropyloxamate (IpOHA) and 2-(dimethylphosphinoyl)-2-hydroxyacetic acid (HOE 704) proved to be tight-binding and competitive inhibitors of the bacterial (*13*, *14*) and plant (*15*, *16*) acetohydroxy acid isomeroreductase. Despite the extremely high overall affinity of these compounds, the second-order rate constants for association of IpOHA and HOE 704 with the plant enzyme are very low, $1.9 \times 10^3$ and $2.2 \times 10^4$ $M^{-1}$ $s^{-1}$, respectively (*15*, *16*). Since inhibition of acetohydroxy acid isomeroreductase leads in vivo to an increase in the acetohydroxy acid substrate concentration (*14*, *17*), these slow-binding competitive inhibitors bind to the

† This study has been supported by the CEA and the BIO AVENIR programme financed by Rhône-Poulenc with the contribution of the Ministère de la Recherche et de l'Espace and the Ministère de l'Industrie et du Commerce Extérieur.

* Corresponding author. Telephone: +(33) 4 72 85 22 96. Fax: +(33) 4 72 85 22 97.

‡ Laboratoire de Spectrométrie de Masse des Protéines, Institut de Biologie Structurale Jean-Pierre Ebel.

§ Laboratoire Mixte CNRS/Rhône-Poulenc (UMR 41), Rhône-Poulenc Agrochimie.

|| Laboratoire de Cristallographie Macromoléculaire, Institut de Biologie Structurale Jean-Pierre Ebel.

⊥ Laboratoire d'Enzymologie Moléculaire, Institut de Biologie Structurale Jean-Pierre Ebel.

# Laboratoire de Synthèse Organique, Rhône-Poulenc Agrochimie.

@ F.V. and F.H. contributed equally to this work.

[1] Abbreviations: AHB, 2-aceto-2-hydroxybutyrate; CID, collision-induced dissociation; ESI, electrospray ionization; HOE 704, 2-(dimethylphosphinoyl)-2-hydroxyacetic acid; $IC_{50}$, concentration of inhibitors yielding 50% inhibition of enzyme activity in the standard protocol given in Experimental Procedures; IpOHA, *N*-hydroxy-*N*-isopropyloxamate; LC, liquid chromatography; MCA, multichannel acquisition; MS, mass spectrometry; nanoESI, nanoelectrospray ionization; MS−MS, tandem mass spectrometry; TFA, trifluoroacetic acid.

S0006-2960(97)02138-7 CCC: $15.00 
Published on Web 03/17/1998

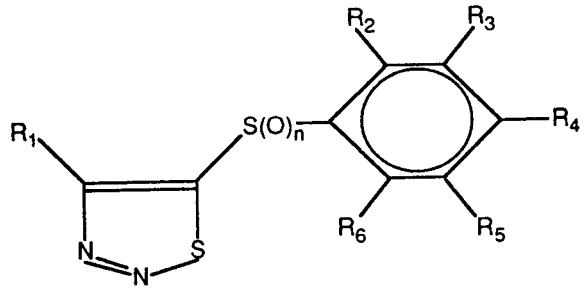


FIGURE 1: Structure of thiadiazole derivatives inhibiting plant acetohydroxy acid isomeroreductase. For compound **1**, $R_1 = COOC_2H_5$, $R_2 = R_3 = R_5 = R_6 = H$, $R_4 = Cl$, and $n = 2$. For compound **2**, $R_1 = COOC_2H_5$, $R_2 = R_3 = R_4 = R_5 = H$, $R_6 = Cl$, and $n = 1$.

enzyme considerably slower as the substrate concentration increases. This mechanism would account for the observation that herbicidal activity is only obtained at a high dose rate for HOE 704 and IpOHA (*15*, *16*).

These findings prompted us to characterize new inhibitors of acetohydroxy acid isomeroreductase that exhibit different mechanisms of inhibition compared with that of the competitive slow-binding transition state analogues discussed above. We report here the results of an in vitro high-throughput screening of diverse molecules on the purified plant acetohydroxy acid isomeroreductase. With this technique, a series of heterocyclic sulfur compounds belonging to the thiadiazole family were found to inhibit noncompetitively the plant enzyme, either reversibly or irreversibly. The binding site on the enzyme was further characterized by mass spectrometry.

## EXPERIMENTAL PROCEDURES

*Materials.* Poly(propylene glycol) and magnesium sulfate were purchased from Aldrich. Endoproteinases ArgC, GluC, and AspN and prolylendoprotease were purchased from Boehringer Mannheim. NADPH was purchased from Sigma. Spinach chloroplast acetohydroxy acid isomeroreductase was cloned and overproduced in *E. coli* following a procedure previously described (*7*).

*Activity Measurements.* Activity measurements were carried out in 96-well microtiter plates. Plates were first incubated in a solution of 0.5% (v/v) Tween 20 (Sigma) for 30 min to prevent unspecific adsorption of enzyme. Then, they were dried and used for the micro-enzyme assays as follows. In each well, the enzyme (10 pmol on a per subunit basis) was preincubated for 10 min at 25 °C in Tris-HCl buffer (pH 8.2) with $Mg^{2+}$ (5 mM), NADPH (500 $\mu$M), and a compound to be analyzed (which was, except where otherwise noted, at a concentration on the order of 2 $\mu$M). The reactions were then initiated by adding the 2-aceto-2-hydroxybutyrate (AHB) substrate (600 $\mu$M), and the kinetics of absorbance changes at 340 nm (oxidation of NADPH; $\epsilon = 6250\ M^{-1}\ cm^{-1}$) were simultaneously recorded for 10 min in the 96 wells by using a microplate reader (Bioteck EL340) driven by a Macintosh IIcx computer equipped with the Delta Soft software (BioMetallics, Inc.). Final reaction volumes were 200 $\mu$L. Except for experiments carried out in the presence of slow-binding inhibitors, kinetics were linear for 20 min, demonstrating adherence to steady state conditions. Nonlinear regression analyses of kinetic data and rate plots were effected by using the Kaleidagraph program (Abelbeck Software). A different protocol was used for kinetic analysis of slow-binding inhibitors. In this case, the enzyme was first preincubated as above with $Mg^{2+}$ and NADPH. Then, the reactions were initiated by adding simultaneously the AHB substrate and the inhibitor. Kinetic data was analyzed as previously described (*18*, *19*).

*Preparation of the Enzyme Complexes for Mass Spectrometric Analyses*. The enzyme−inhibitor (compound **1**, Figure 1) complex was obtained by sequential addition of 1 nmol of the enzyme, 5 nmol of $Mg^{2+}$ and NADPH, and 1 nmol of compound **1** [dissolved in 3% acetone (v/v)] in a final volume of 50 $\mu$L in 10 mM ammonium acetate (pH 8.2). The complex was allowed to form by incubation for 35 min at 20 °C. To check the specificity of thiadiazole inhibitor binding, a synthetic peptide (MLSLRQSIRFFK-PATRTLCSSRYLL) containing a single free cysteine was submitted to alkylation for 15 min at 20 °C with a molar ratio of compound **1**.

*ESI-MS Analyses*. The mass spectra were acquired on a Sciex API III+ triple quadrupole mass spectrometer (Perkin-Elmer Sciex) equipped with a nebulizer-assisted electrospray (ion spray) source. The instrument was calibrated using poly(propylene glycol). The ion spray probe tip was held at 5 kV, and the orifice voltage was set at 90 or 60 V for protein or peptide analyses, respectively. For the flow injection analyses, proteins were infused with 25% methanol and 1% acetic acid into the source using a Harvard 22 syringe pump (Touzart & Matignon) at a flow rate of 5 $\mu$L $min^{-1}$. For acetohydroxy acid isomeroreductase, the mass spectra were acquired in the 1400−2400 range of mass-to-charge (*m*/*z*) ratios in steps of 0.9 *m*/*z*, with a 2 ms dwell time. For peptides, scans were acquired from *m*/*z* 400 to 1400 with a 0.5 *m*/*z* step with 2 ms per step. Tandem MS experiments were performed using a nanoelectrospray (nanoES) source built in house, according to a method previously described (*20*). The peptide mixture (2 $\mu$L) obtained from AspN digestion of the enzyme−inhibitor complex was purified using a $C_8$ microcolumn and loaded into the needle. Collision-induced dissociation (CID) spectra were acquired from *m*/*z* 100 to 1500 with a 0.5 *m*/*z* step with a dwell time of 2 ms in the multichannel acquisition (MCA) mode to improve the signal-to-noise ratio. Mass spectra were analyzed using a Quadra 950 data system (Apple Computer Inc.), and molecular masses were calculated using the MacSpec Software (Perkin-Elmer Sciex).

*Enzymatic Digestion of the Enzyme−Inhibitor Complex and LC−MS Analyses.* One nanomole of the acetohydroxy acid isomeroreductase−compound **1** complex was digested overnight in the presence of various endoproteinases (AspN, ArgC, and GluC) in 50 $\mu$L of a 10 mM ammonium acetate solution (pH 8.8) at 37 °C and a protease/substrate ratio of 1/60 (w/w). After digestion, peptide mixtures were separated with a homemade $C_8$ column (0.25 mm × 100 mm) using a 140B solvent delivery system and a 785A absorbance detector (Applied Biosystems). The flow rate was 5 $\mu$L $min^{-1}$ with a linear gradient of 5 to 55% acetonitrile (in 0.1% TFA) over the course of 55 min. The entire flow was directed to the mass spectrometer, and peptide elution was followed using the absorbance of the peptidic bond at 214 nm. Numbering of the peptide sequences is as defined for the mature plant enzyme without the 72 amino acids of the transit peptide (*6*).

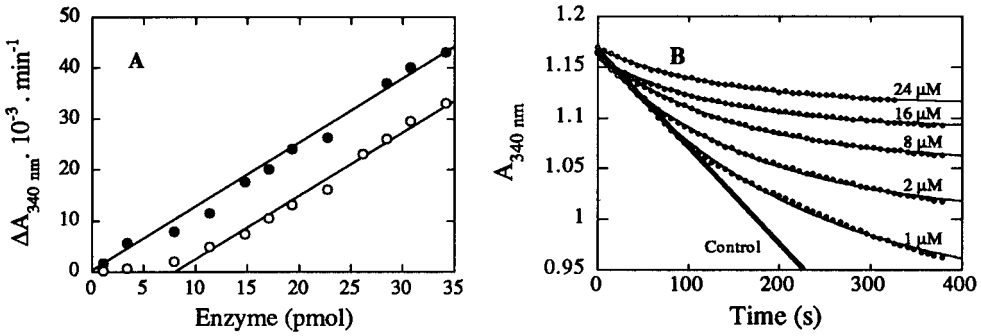


FIGURE 2: Kinetics of irreversible inhibition of plant acetohydroxy acid isomeroreductase by compound **1**. (A) Dependence of the rate of NADPH oxidation on the enzyme concentration in the absence (●) or presence (○) of 7 pmol of compound **1**. (B) Progressive inhibition of enzyme-catalyzed NADPH oxidation in the presence of different concentrations of compound **1** as indicated on the plots. The curves show the best fits to eq 3, allowing the determination of $k_{obs}$, the pseudo-first-order rate constant for inhibition. The straight line (control) corresponds to the NADPH oxidation catalyzed by the enzyme in the absence of compound **1**.

*Edman Degradation.* The amino acid sequence of the alkylated peptide of acetohydroxy acid isomeroreductase was also determined by Edman degradation using a sequenator (model 477A, Applied Biosystems) coupled to an on-line PTH-amino acid analyzer (model 120A, Applied Biosystems). A synthetic peptide (MLSLRQSIRFFKPATRTLCSSRYLL) was used to obtain standard retention times of alkylated cystein. After alkylation by compound **1**, the modified peptide was digested by prolylendopeptidase [45 min, 50 mM ammonium acetate (pH 7.0) at 20 °C with an enzyme/substrate ratio of 1/1000] to obtain a shorter peptide (ATRTLCSSRYLL) with a more suitable position for Edman degradation sequencing of cysteine. After separation of the alkylated peptide on a $C_8$ reverse phase column (2.1 mm × 100 mm) using a linear gradient of 9 to 63% (v/v) acetonitrile in water (0.1% TFA), peptide fractions were analyzed by MS and the purified alkylated peptide was submitted to 10 cycles of Edman degradation.

## RESULTS

A microassay was developped as described in Experimental Procedures to allow the screening of a large number of molecules on the activity of recombinant spinach chloroplast acetohydroxy acid isomeroreductase. Consistent with previous results (*7*), initial experiments confirmed a sequential ordered mechanism for the plant enzyme-catalyzed reaction, in which NADPH and $Mg^{2+}$ bind first and independently to the enzyme, and acetohydroxy acid substrate binds second. Furthermore, the enzyme exhibited Michaelis−Menten behavior with respect to all substrates and cofactors, yielding $K_m$ values for AHB, $Mg^{2+}$, and NADPH of 10, 5, and 5 $\mu$M, respectively, also in agreement with previous results (*7*). With this technique, about 10 000 different molecules were assayed, out of which several heterocyclic sulfur compounds belonging to the family of thiadiazoles (Figure 1) were found to strongly inhibit the plant enzyme, either irreversibly (e.g. compound **1** in Figure 1) or reversibly (e.g. compound **2** in Figure 1). The mechanism of inhibition by these two compounds was assessed by steady state kinetic measurements.

*Compound **1** Is an Irreversible Noncompetitive Inhibitor of Plant Acetohydroxy Acid Isomeroreductase.* In agreement with previous results (*15*), the rate plot of $v$ (steady state rate of NADPH oxidation) versus the concentration of the enzyme in the assay was linear in the range of 0−35 pmol of enzyme, demonstrating adherence to steady state conditions. Figure 2A shows that this rate plot had the same slope in the presence of 7 pmol of compound **1** as it did in its absence. However, this plot did not pass through the origin but instead yielded a horizontal axis intercept corresponding to 7 pmol of enzyme (on a per subunit basis). These features are characteristic of tight-binding inhibition (*21*, *22*). Furthermore, these data show that a molar ratio of inhibitor/enzyme of 1/1 was sufficient to provide complete inhibition of enzyme activity, suggesting a stoichiometric binding of compound **1** to the plant acetohydroxy acid isomeroreductase. Thus, compound **1** acts as an affinity label in inactivating the enzyme.

Inhibition of enzyme activity by compound **1** was time-dependent (Figure 2B). Therefore, the mechanism of inhibition was characterized by investigating the effect of substrate and inhibitor concentrations on the time dependence of inhibition (*18*, *19*). When the plant enzyme was assayed in the simultaneous presence of substrate and inhibitor, nonlinear time courses of NADPH oxidation were observed (Figure 2B). At high inhibitor concentrations, the inhibition was nearly complete, suggesting that compound **1** behaved as a nearly irreversible inhibitor of the plant enzyme, in agreement with the data in Figure 2A. For the formation of an encounter complex between enzyme (E) and inhibitor (I)

$$E + I \underset{k_{-0}}{\overset{k_0}{\rightleftharpoons}} E{-}I \qquad (1)$$

If the inhibitor reacts slowly with the enzyme, and E−I is catalytically inactive, then product formation should approach an asymptote:

$$[P] = [P]_\infty(1 - e^{-k_{obs}t}) \qquad (2)$$

where [P] and $[P]_\infty$ are, respectively, the concentrations of product formed at time $t$ and at time approaching infinity and $k_{obs}$ is the pseudo-first-order rate constant for inhibition. Since product formation was measured by monitoring the decrease in absorbance at 340 nm due to NADPH oxidation, eq 2 becomes

$$A_{340}^t = A_{340}^\infty + (A_{340}^0 - A_{340}^\infty)e^{-k_{obs}t} \qquad (3)$$

where $A_{340}^t$, $A_{340}^0$, and $A_{340}^\infty$ are the absorbance at 340 nm at time $t$, at time zero, and at time approaching infinity,

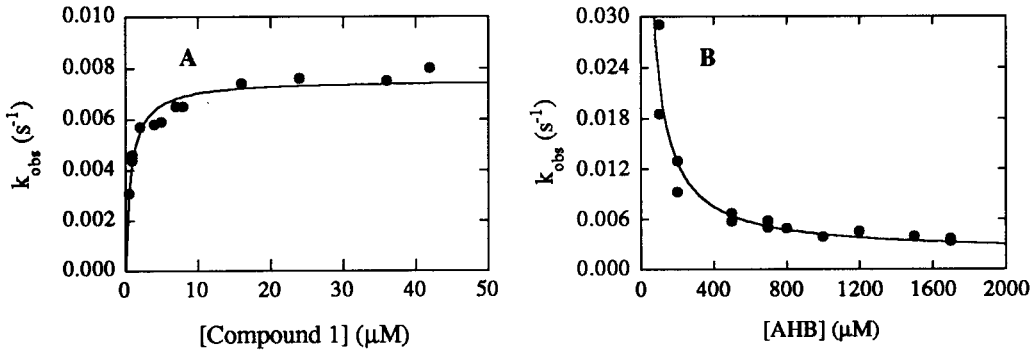


FIGURE 3: Kinetics of interaction of plant acetohydroxy acid isomeroreductase with compound **1**. (A) Dependence of the pseudo-first-order rate constant for inhibition, $k_{obs}$, on the concentration of compound **1**. The curve shows the best fit to eq 5 describing the binding, which yielded the $K_{app}$ value for reversible association of compound **1** to enzyme ($K_{app} = 0.75 \pm 0.11$ μM) and the $k$ value for the formation of the irreversible enzyme−compound **1** complex ($k = 0.0075 \pm 0.00019$ $s^{-1}$). (B) Dependence of the pseudo-first-order rate constant for inhibition, $k_{obs}$, on the concentration of acetohydroxy acid substrate, AHB. The curve shows the best fit to eq 6, which yielded the following values of the $p_1-p_3$ parameters: $p_1 = 0.0019 \pm 0.0009$ $s^{-1}$, $p_2 = 2.32 \pm 0.27$ μM $s^{-1}$, and $p_3 = 10.1 \pm 2.2$ μM.

respectively. As shown in Figure 2B, the experimental time courses could be fitted satisfactorily by using eq 3 and a nonlinear least-squares program, allowing the determination of $k_{obs}$.

For an inhibition occurring without prior formation of a reversible intermediate enzyme−inhibitor complex (eq 1), $k_{obs}$ is a linear function of [I], the inhibitor concentration (*19*). That is, $k_{obs} = k_0[I] + k_{-0}$. On the other hand, for an irreversible inhibition occurring through prior formation of a reversible intermediate enzyme−inhibitor complex,

$$E + I \underset{k_{-0}}{\overset{k_0}{\rightleftharpoons}} E{-}I \xrightarrow{k} E{-}I^* \qquad (4)$$

the representation of $k_{obs}$ versus [I] is a hyperbola (*19*). In this case,

$$k_{obs} = \frac{k[I]}{K_{app} + [I]} \qquad (5)$$

where $K_{app} = k_{-0}/k_0$.

The data of Figure 3A show that a plot of $k_{obs}$ versus [compound **1**] was not linear, indicating that enzyme inactivation proceeded through the formation of a reversible enzyme−inhibitor complex, as depicted in eq 4.

At a fixed concentration of compound **1** of 10 μM, the value of $k_{obs}$ was not dependent on $Mg^{2+}$ or NADPH concentration, indicating that the binding of compound **1** to the plant enzyme did not interfere with that of the metal ion cofactor and nucleotide substrate (data not shown). In contrast, $k_{obs}$ was dependent on the acetohydroxy acid substrate concentration (Figure 3B). These data could be fitted to a decreasing hyperbola:

$$k_{obs} = \frac{p_1[AHB] + p_2}{[AHB] + p_3} \qquad (6)$$

In contrast to the behavior expected for a competitive inhibitor, $k_{obs}$ did not approach zero at very high acetohydroxy acid substrate concentrations, but instead reached a finite limiting value (Figure 3B). A model simpler than eq 6 above, in which the value of $p_1$ was set to zero, was eliminated because the fit was rather poor, especially in the high AHB concentration range. Thus, enzyme inhibition by compound **1** cannot be totally alleviated by the presence of excess acetohydroxy acid substrate. This suggests that a complex composed of enzyme, $Mg^{2+}$, NADPH, AHB, and inhibitor exists. A mechanism consistent with these results is as follows (Scheme 1):

Scheme 1

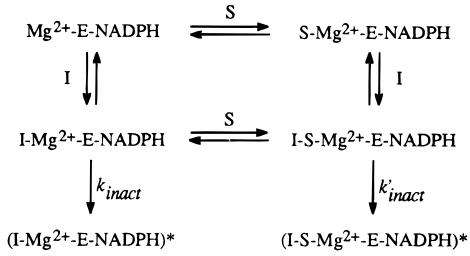


in which E stands for enzyme, I for compound **1**, and S for acetohydroxy acid substrate and $k_{inact}$ and $k'_{inact}$ refer to the inactivation rate constants of enzyme−$Mg^{2+}$−inhibitor−NADPH and enzyme−$Mg^{2+}$−inhibitor−NADPH−AHB complexes, respectively. Furthermore, the observed dependence of $k_{obs}$ on the concentration of AHB substrate (Figure 3B) suggests that the enzyme−$Mg^{2+}$−NADPH−AHB complex can be irreversibly inhibited by compound **1** at a slower rate than the enzyme−$Mg^{2+}$−NADPH complex.

*Compound **2** Is a Reversible Noncompetitive Inhibitor of Plant Acetohydroxy Acid Isomeroreductase*. In the presence of compound **2** (see Figure 1), the rate plot of $v$ (steady state rate of NADPH oxidation) versus the concentration of the enzyme in the assay was linear in the range of 0−150 pmol of enzyme (Figure 4A). However, the slope of this plot was smaller than that obtained in the absence of inhibitor and, furthermore, yielded a zero intercept (Figure 4A). This behavior indicates, therefore, that compound **2** acts as a reversible inhibitor of plant acetohydroxy acid isomeroreductase (*22*). This allowed the determination of the mechanism of inhibition to be assessed by steady state rate measurements in which two of the substrate cofactors were held constant at saturating concentrations, whereas the third one was varied, either in the absence or in the presence of fixed amounts of compound **2**.

When AHB and $Mg^{2+}$ concentrations were fixed at 0.6 and 5 mM, respectively, and that of NADPH was varied in the range of 4−16 μM, linear parallel double-reciprocal rate

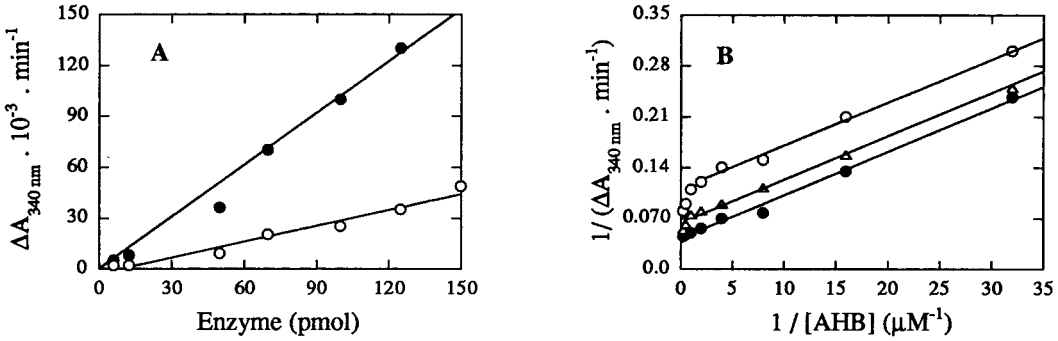


FIGURE 4: Kinetics of reversible inhibition of plant acetohydroxy acid isomeroreductase by compound **2**. (A) Dependence of the rate of NADPH oxidation on the enzyme concentration in the absence (●) or presence (○) of 50 pmol of compound **2**. (B) Double-reciprocal plots of 1/(velocity of NADPH oxidation) versus 1/[acetohydroxy acid substrate] in the absence (●) or presence of 10 $\mu$M (○) or 100 $\mu$M (○) compound **2**.

plots of $1/v$ versus 1/[NADPH] were obtained in the absence and presence of compound **2**. The same pattern of behavior was observed with $Mg^{2+}$ as was observed with the varied cofactor (data not shown), indicating that compound **2** behaves as an uncompetitive inhibitor with respect to NADPH and $Mg^{2+}$ (*22*).

A more complex pattern of behavior was observed with AHB as the varied substrate. In agreement with previous results (*7*), in the absence of compound **2**, the double-reciprocal plot of $1/v$ versus 1/[AHB] was linear (Figure 4B). In the presence of compound **2**, however, the plots were curvilinear, exhibiting parallel portions only in the low acetohydroxy acid substrate concentration range (Figure 4B). This pattern is typical of noncompetitive inhibition with respect to AHB (*22*), meaning that compound **2** and AHB bind to the enzyme at different sites to yield enzyme−AHB, enzyme−compound **2**, and enzyme−AHB−compound **2** complexes. A mechanism consistent with these results can be depicted as follows (Scheme 2):

Scheme 2

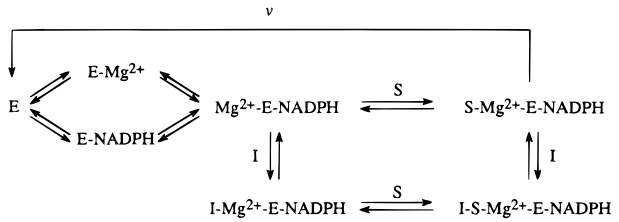


where E stands for the enzyme, S for acetohydroxy acid substrate, and I for compound **2**.

*Structure−Activity Relationships within the Thiadiazole Family*. The above data show that members of the thiadiazole family can inhibit the plant acetohydroxy acid isomeroreductase to different extents. Besides compounds **1** and **2** characterized above, we have also analyzed 138 other derivatives in this family, which were classified according to their $IC_{50}$ values (i.e. the concentrations of inhibitors yielding 50% inhibition of enzyme activity in the standard protocol given in Experimental Procedures). A survey of these results indicated that essentially two factors can affect the $IC_{50}$ values. The first one concerns the oxidation state of the sulfur atom bridging the two cycles in the molecules (Figure 1). The $IC_{50}$ values increased in the following order: sulfone ($SO_2$) < sulfoxyde (SO) < sulfur (S). The other one relates to the electrophilicity of the thiadiazole ring, since the $IC_{50}$ values decreased greatly as the electrophilicity of the $R_1$ group (Figure 1) increased. Other factors, such as the lipophilicity and size of the molecules, did not affect the $IC_{50}$ values significantly.

*Mass Spectrometric Analyses of the Enzyme−Compound **1** Complex*. The above kinetic studies indicated that compound **1** behaves like an irreversible inhibitor of the plant acetohydroxy acid isomeroreductase. The binding site appeared to be different from that previously characterized for the transition state analogue, IpOHA, which inhibits the enzyme in a competitive manner with respect to the acetohydroxy acid substrate (*15*, *16*). To obtain structural information on this binding site, mass spectrometry analyses of the enzyme−compound **1** complex were carried out. Comparison of the mass spectra of the free enzyme and of the enzyme−compound **1** complex revealed a mass increase of 158 ± 3 Da for the enzyme−compound **1** complex (Figure 5A). Furthermore, the denaturing conditions used to acquire this spectrum indicated a covalent nature of the complex. As this increase in mass did not fit with the expected mass of compound **1** (332.8 Da), this result indicates that a portion of the inhibitor molecule was released during its binding to the enzyme. For an equimolar ratio of inhibitor to protein, reconstructed molecular mass profiles showed approximately 20% of free enzyme and 60% of enzyme with one inhibitor molecule bound (Figure 5B). Four additional minor peaks (ca. 5% each) were present with a mass increase of 318, 474, 632, and 790 Da, corresponding to the binding of two (E + 2I), three (E + 3I), four (E + 4I), and five (E + 5I) inhibitor molecules per enzyme subunit, respectively (Figure 5B). Essentially similar data were obtained when the complex was generated in the presence of $Mg^{2+}$ and/or NADPH (data not shown).

To identify the inhibitor binding site, the enzyme−compound **1** complex was digested with endoproteinases AspN, ArgC, and GluC, and the resulting peptide mixtures were analyzed by LC−ESI-MS. For all digestions, the mass spectra disclosed one main peptide modified by the inhibitor (Table 1). From these data, the major binding site of the inhibitor was located between amino acids 494 and 502 of the plant protein.

The peptide of residues 493−505 was isolated from endoproteinase AspN digestion of the enzyme−compound **1** complex. This peptide was submitted to sequence determination by Edman degradation. This analysis gave the sequence EAIGVXAQLRPSV, in agreement with the amino

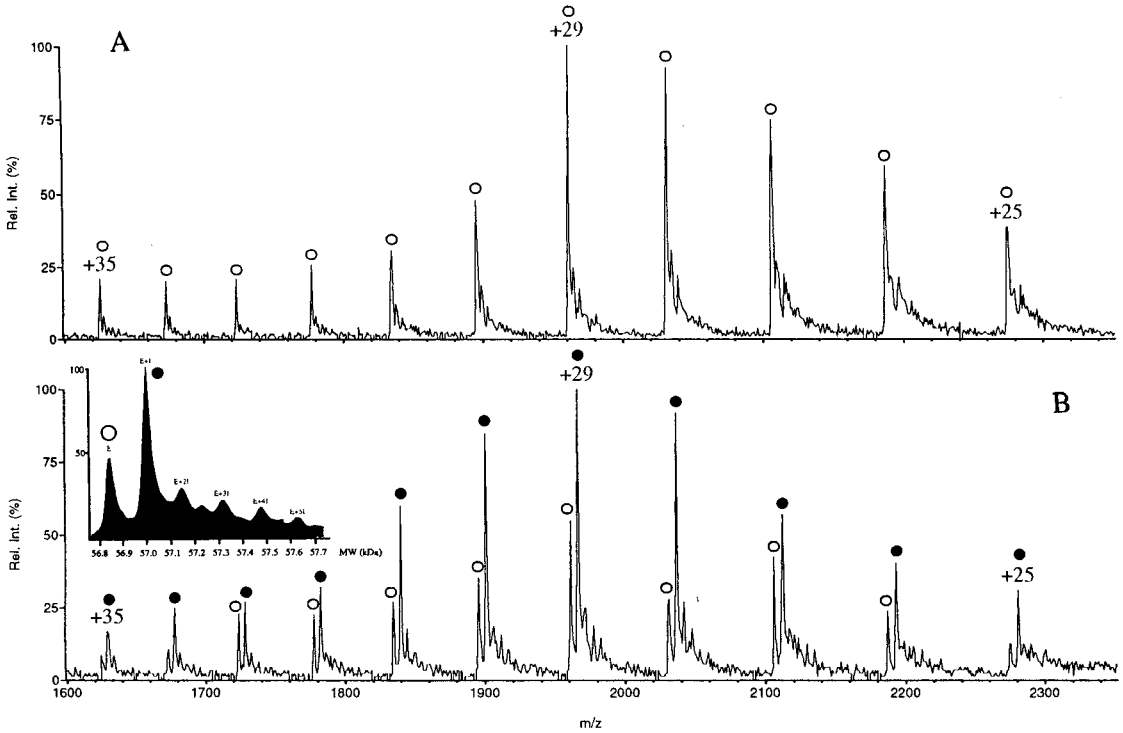


FIGURE 5: Mass spectra of native acetohydroxy acid isomeroreductase and of the enzyme−compound **1** complex (for conditions and analysis, see Experimental Procedures). (A) Native enzyme showing a mass of 56 853 ± 3 Da. (B) Enzyme−compound **1** complex showing a mass of 57 011 ± 3 Da. The peaks that correspond to the enzyme−compound **1** complex and to the free enzyme are labeled with filled and open circles, respectively. From the ESI-MS reconstructed molecular mass profile, the major peak corresponding to the enzyme−compound **1** complex represents about 60% of the total enzyme.

Table 1: Identification of Peptides Carrying the Inhibitor Issued from Digestion of the Acetohydroxy Acid Isomeroreductase−Compound **1** Complex by Various Endoproteinases

| proteases | localization | $\Delta m^a$ (Da) |
|---|---|---|
| AspN | 493−505 | 157 |
| GluC | 494−519 | 158 |
| ArgC | 455−502 | 157 |

[a] $\Delta m$ = mass increase due to the inhibitor binding.

acid sequence deduced from the cDNA encoding spinach chloroplast acetohydroxy acid isomeroreductase (*6*) (from the latter, X corresponds to Cys498). As the detection of free cysteine residues by Edman degradation is known to be difficult and as the PTH-derivatized of cysteine alkylated with compound **1** was not detected by this technique, we could not ascertain the nature of residue X. We tried to clarify this ambiguity by using a single free cysteine synthetic peptide alkylated with compound **1**, but again, no PTH-alkylated cysteine was detected. These results, however, testify to the absence of adduct formation between compound **1** and any other putative reactive amino acid like arginine or lysine.

The sequence of the 493−505 peptide resulting from AspN digestion of the plant enzyme−compound **1** complex was also determined by tandem mass spectrometry using a nanospray ion source. After selection of the doubly charged ion (*m*/*z* 750) of the 493−505 peptide (1498 Da), this ion was fragmented in the collision cell and the fragments were analyzed (Figure 6). Most of the fragments were B and Y″ ions resulting from peptide bond cleavages. Other cleavages were also seen, such as A and C or X″ and Z ions corresponding to additional fragmentations from the N or C terminus part, respectively (*23*). On the basis of a comparison of theoretical masses of the fragment ions with those of the CID spectra, the amino acid sequence of the peptide was determined. This sequence was in good agreement with that deduced from the cloned cDNA encoding the enzyme (*6*). Furthermore, ions with an increase in mass of 157 Da (labeled with an asterisk in Figure 6) allowed us to identify Cys498 as the amino acid residue of the protein that was modified upon compound **1** adduct formation.

The specificity of compound **1** binding to Cys498 of the plant enzyme was assessed further by conducting binding experiments with a single-cysteine-containing synthetic peptide (MLSLRQSIRFFKPATRTLCSSRYLL) of unrelated sequence compared with that of the 493−505 peptide produced by endoproteinase AspN digestion of the enzyme−compound **1** complex (see Experimental Procedures). MS analysis showed that a complex formed between the synthetic peptide and compound **1**, characterized by an increase in mass of 157 ± 0.3 Da, similar to that observed for the plant enzyme−compound **1** complex. For a synthetic peptide/inhibitor ratio of 1/1, the peptide−inhibitor complex formed accounted for ca. 75% of the total amount of peptide in the assay (data not shown). This strongly suggests that compound **1** may potentially react with any of the cysteine residues present in the acetohydroxy acid isomeroreductase. The fact, however, that adduct formation occurred mainly at Cys498 of the protein suggests that the inhibitor had preferential access to this residue in the native protein. The enzyme crystal structure (*12*) reveals that Cys498 is located in a cleft between the N- and the C-terminal domains of acetohydroxy acid isomeroreductase. Figure 7 shows the location of this cysteine and a blowup of the area binding,

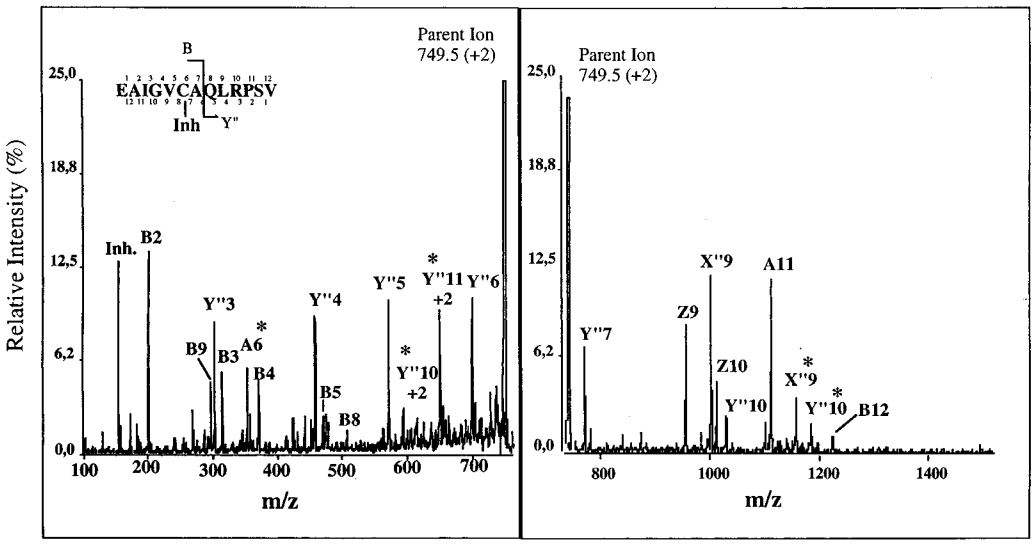


FIGURE 6: NanoES tandem mass spectra of the 1498.2 Da peptide (referred to as the 493−505 peptide), obtained from digestion of the acetohydroxy acid isomeroreductase−compound **1** complex with endoproteinase AspN (for conditions and analysis, see Experimental Procedures). Peaks labeled with an asterisk correspond to fragments modified by compound **1** adduct formation (mass increase of 157 Da). Extensive release of the inhibitor during acquisition occurred as only few modified fragments were found for most of the monocharged ions (Z9, X″9, A11, ...). Uncommon fragmentations were due to the drastic conditions used to sequence such peptides containing an acidic residue at its N terminus. A, X, and other fragments were attributed to the presence of the inhibitor.

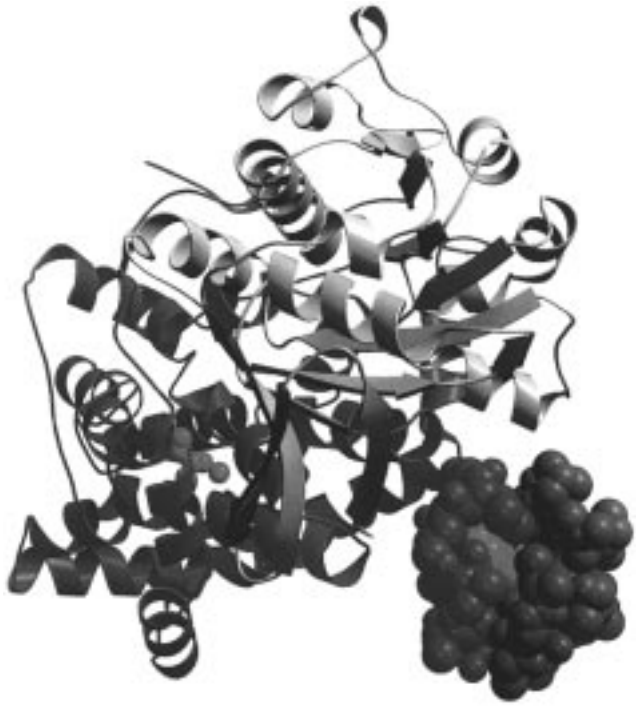

FIGURE 7: Crystal structure of the spinach chloroplast acetohydroxy acid isomeroreductase−NADPH−$Mg^{2+}$−IpOHA complex (*12*). N- and C-terminal domains are gray and blue, respectively, and Cys498 is in red. Also shown is a blowup of the protein region surrounding the Cys498 residue.

demonstrating that Cys498 is vulnerable to compound **1** attack at the bottom of this cleft. This figure also shows that the active site is at the interface between N- and C-terminal domains, but is located about diametrically opposite of Cys498.

## DISCUSSION

These results demonstrate the possibility of discovering new inhibitors of a plant acetohydroxy acid isomeroreductase, different from the previously characterized transition state analogues that bind competitively with respect to the acetohydroxy acid substrate (*13*−*16*). Thus, after a number of unrelated molecules were screened, heterocyclic sulfur compounds related to the thiadiazole family were found to inhibit strongly the plant enzyme in a noncompetitive manner.

The members of the thiadiazole inhibitor family fall into two categories depending on whether they bind irreversibly (e.g. compound **1**; Figure 1) or reversibly (e.g. compound **2**; Figure 1) to the plant enzyme. From a mass spectrometric analysis of peptides produced by the action of various proteases on the enzyme−compound **1** complex, the binding site of this inhibitor was located in the C-terminal portion of the enzyme. In an attempt to identify which amino acid residue interacts with the inhibitor, tandem MS experiments were carried out to deduce the sequence of the main modified peptide, i.e. the 493−505 peptide obtained from AspN digestion of the enzyme−compound **1** complex. We have used a nanoES source, built in our laboratory according to a method previously described (*20*). This technique was of particular interest in this work because the flow rate sample directed to the MS is around 30−50 nL/min. Therefore, the CID spectra can be acquired for a long time, which improved the signal-to-noise ratio. This allowed an accurate determination of Cys498 being the site where adduct formation mainly occurred. From the known crystal structure of the plant acetohydroxy acid isomeroreductase (*12*), it is clear that this residue is located away from the enzyme active site, again confirming the noncompetitivity of the inhibitors analyzed here (Figure 7).

The kinetic results show that both inhibitor classes exhibit the same type of primary interaction with the enzyme. That is, the irreversible compound binds the enzyme through a reversible bimolecular step, which exhibits the same characteristics with respect to acetohydroxy acid substrate, coenzyme, and metal ion cofactor as the binding step involving the reversible inhibitor. This suggests strongly that

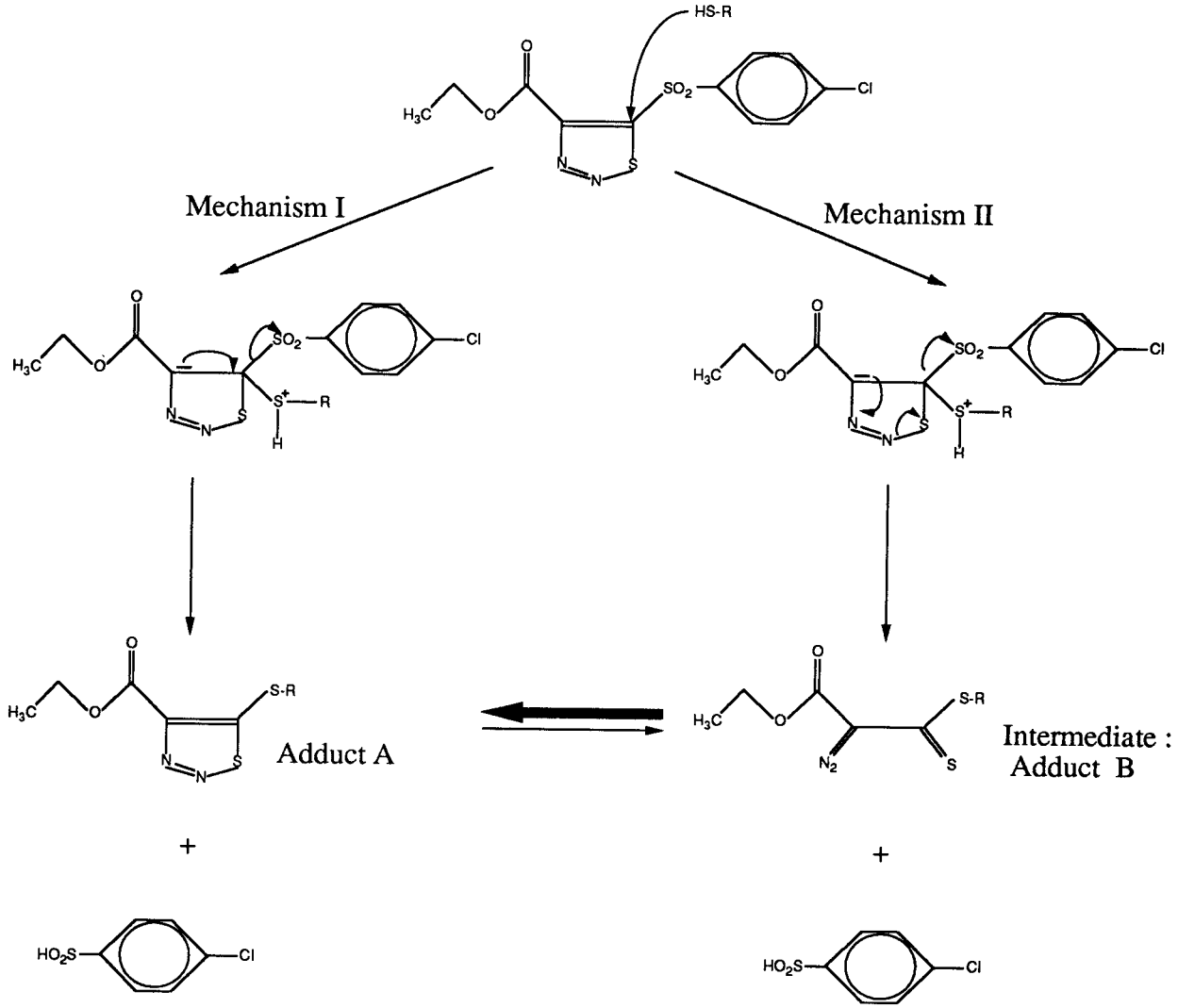


FIGURE 8: Proposed reaction mechanism for adduct formation between compound **1** and Cys498 (R−SH) of plant acetohydroxy acid isomeroreductase. After Michael addition of the sulfhydryl of Cys498 to the α,β unsaturated double bond, the elimination of the sulfinic acid can be obtained by two mechanisms (I and II). In both cases, the adducts have a mass of 157 Da. However, addduct **B** is known as an unstable transient intermediate which further leads to compound **A**.

(i) both reversible and irreversible inhibitors of the thiadiazole family can specifically recognize a particular binding site on the enzyme and (ii) only for the irreversible inhibitor can a particular amino acid residue located in this specific protein pocket (i.e. Cys498) react further, thus leading to irreversible adduct formation and allowing us to label the inhibitor binding site. The cause of enzyme inhibition by compound **1**, therefore, does not appear to be adduct formation with Cys498 but primary interaction with a binding site on the enzyme proximal to this residue.

An analysis of the data in Figure 3B indicates that compound **1** can react with both the enzyme−$Mg^{2+}$−NADPH and enzyme−$Mg^{2+}$−NADPH−AHB complexes. Furthermore, the pseudo-first-order rate constant, $k_{obs}$, for inhibition of the enzyme by compound **1** displayed a strong dependence on acetohydroxy acid substrate concentration. The data could be well fitted using a decreasing hyperbola (eq 6, Figure 3B). The parameter $p_3$ of eq 6 can give a measure of the interaction of the enzyme−NADPH−$Mg^{2+}$−compound **1** complex with the AHB substrate. Nonlinear regression analyses disclosed that the best-fit value of $p_3$ (10 ± 2 μM) was similar to the $K_m$ value of the enzyme for the AHB substrate in the absence of compound **1** (10 μM; this study and ref *7*). Assuming pseudo-equilibrium conditions, microscopic reversibility implies that the equilibrium constants for the reversible step of compound **1** binding to the enzyme−$Mg^{2+}$−NADPH and enzyme−$Mg^{2+}$−NADPH−AHB complexes (see Scheme 1) also have similar values, again in agreement with the noncompetitive character of the inhibition process. An analysis of eq 6 and of the best-fit parameters $p_1$ and $p_2$ also allows us to put limits on some of the rate constants in Scheme 1. Thus, from the data in Figure 3B and eq 6, a limiting value of $k_{inact}$, the unimolecular rate constant for inactivation of the enzyme−$Mg^{2+}$−NADPH−compound **1** complex, is given by the ratio $p_2/p_3$. The value of $k_{inact}$ calculated in this manner is 0.23 $s^{-1}$ (see Figure 3B), corresponding to a $\tau_{1/2}$ value of about 3 s. On the other hand, a limiting value of $k'_{inact}$, the unimolecular rate constant for inactivation of the enzyme−$Mg^{2+}$−NADPH−AHB−compound **1** complex is given by $p_1$ (eq 6). From the data in Figure 3B, the best-fit value of $k'_{inact}$ is 0.002 ± 0.0009 $s^{-1}$, corresponding to a $\tau_{1/2}$ value of about 6 min. This 100-fold difference between the values of $k_{inact}$ and $k'_{inact}$ indicates, therefore, that irreversible inhibition of the enzyme by compound **1** occurs at a much faster rate in the absence than in the presence of the acetohydroxy acid substrate. This

finding suggests that the binding of the acetohydroxy acid substrate induces a conformational change in the enzyme so that the accessibility and/or the reactivity of the Cys498 residue is altered. The occurrence of conformational changes of the enzyme was previously documented from spectroscopic measurements showing that the fluorescence of enzyme-bound NADPH is markedly affected by the binding of the IpOHA or AHB substrate to the enzyme (*7*, *15*). On the basis of Figure 3, compound **1** has a maximum rate of inactivation ($k_{inact}$) of 0.23 $s^{-1}$ and an inactivation constant ($K_{app}$) of 0.75 $\mu$M, giving it a second-order rate constant for interaction with the enzyme at low inhibitor concentrations ($k_{inact}/K_{app}$) of $3 \times 10^5$ $M^{-1}$ $s^{-1}$. This value is 150-fold higher than that for IpOHA binding to the enzyme (*10*). Thus, compound **1** reaches its target site at a faster rate than the active site-directed IpOHA.

ESI-MS experiments indicated that a major enzyme species presents an increase in mass of 158 ± 3 Da upon binding of compound **1** (Figure 5). As this mass increase differs from the molecular mass of compound **1** (332.8 Da), a release of part of the inhibitor must have occurred during adduct formation. Assuming a nucleophilic attack on position $C_5$ of the thiadiazole ring of compound **1**, that attack would lead to a mass increase of 157.1 Da for the protein−inhibitor adduct, a value that is very close to that determined experimentally for complexes of compound **1** with either the plant enzyme (158 + 3 Da) or a cysteine-containing synthetic peptide (157.6 ± 0.5 Da) of unrelated sequence with respect to that of the enzyme. Also, a nucleophilic attack on $C_5$ is consistent with the observed structure−activity relationship among thiadiazole derivatives showing that the higher the electrophilicity of the thiadiazole ring the lower the $IC_{50}$ values. Possible mechanisms of adduct formation are presented in Figure 8. After Michael addition of the sulfhydryl of Cys498 to the $\alpha,\beta$ unsaturated double bond, the elimination of the sulfinic acid can be obtained by mechanisms I and II of Figure 8. In both cases, the adducts have a mass of 157 Da. However, adduct **B** corresponding to the open form (mechanism II) is known as an unstable transient intermediate which further leads to compound **A** (*24*). These mechanisms, which involve nucleophilic attack of compound **1** by a nucleophile from the protein (e.g. Cys498), are further supported by the absence of detection of the isotopic contribution of the chloride atom as the *p*-$ClC_6H_4SO_2$ group is released during the binding of compound **1** (data not shown).

The pocket including Cys498 is located in the C-terminal domain of the protein at the interface between the N- and C-terminal domains (Figure 7). Site-directed mutagenesis and molecular modeling experiments are in progress to characterize further this new site of noncompetitive inhibition of acetohydroxy acid isomeroreductase.

## ACKNOWLEDGMENT

We acknowledge Pierre Génix, Flavien Proust, Philippe Desbordes, Jean-François Hernandez, Isabelle Bally, and Georges Freyssinet for many helpful scientific discussions.

## REFERENCES

1. Shaner, D. L., Anderson, P. C., and Stidham, M. A. (1984) *Plant Physiol. 76*, 545−546.
2. Chaleff, R. S., and Mauvais, C. J. (1984) *Science 224*, 1443−1444.
3. Singh, B. K., and Shaner, D. L. (1995) *Plant Cell 7*, 935−944.
4. Chunduru, S. K., Mrachko, G. T., and Calvo, K. C. (1989) *Biochemistry 28*, 486−493.
5. Dumas, R., Joyard, J., and Douce, R. (1989) *Biochem. J. 262*, 971−976.
6. Dumas, R., Lebrun, M., and Douce, R. (1991) *Biochem. J. 277*, 469−475.
7. Dumas, R., Job, D., Ortholand, J.-Y., Emeric, G., Greiner, A., and Douce R. (1992) *Biochem. J. 288*, 865−874.
8. Dumas, R., Butikofer, M. C., Job, D., and Douce, R. (1995) *Biochemistry 34*, 6026−6036.
9. Dumas, R., Biou, V., and Douce, R. (1997) *FEBS Lett. 40*, 156−160.
10. Dumas, R., Job, D., Douce, R., Pebay-Peroula, E., and Cohen-Addad, C. (1994) *J. Mol. Biol. 242*, 578−581.
11. Biou, V., Pebay-Peroula, E., Cohen-Addad, C., Vives, F., Butikofer, M. C., Curien, G., Job, D., Douce, R., and Dumas, R. (1995) in *Photosynthesis: from light to biosphere* (Mathis, P., Ed.) Vol. 5, pp 335−340, Kluwer, Dordrecht, The Netherlands.
12. Biou, V., Dumas, R., Cohen-Addad, C., Job, D., Douce, R., and Pebay-Peroula, E. (1997) *EMBO J. 16*, 3405−3415.
13. Aulabaugh, A., and Schloss, J. V. (1990) *Biochemistry 29*, 2824−2830.
14. Schulz, A., Spönemann, P., Köcher, H., and Wengenmayer, F. (1988) *FEBS Lett. 238*, 375−378.
15. Dumas, R., Cornillon-Bertrand, C., Guigue-Talet, P., Génix, P., Douce, R., and Job, D. (1994) *Biochem. J. 301*, 813−820.
16. Dumas, R., Vives, F., Job, D., Douce, R., Biou, V., Pebay-Peroula, E., and Cohen-Addad, C. (1995) *Brighton crop protection conference−Weeds*, 7B-3, pp 833−842, British Crop Protection Council.
17. Wittenbach, V. A., Aulabaugh, A., and Schloss, J. V. (1990) in *Pesticide Chemistry* (Frehse, H., Ed.) pp 151−160, VCH, Weinheim.
18. Tian, W.-X., and Tsou, C.-L. (1982) *Biochemistry 21*, 1028−1032.
19. Liu, L., and Tsou, C.-L. (1986) *Biochim. Biophys. Acta 70*, 185−190.
20. Wilm, M., and Mann, M. (1996) *Anal. Chem. 68*, 1−8.
21. Morison, J. F. (1969) *Biochim. Biophys. Acta 185*, 269−286.
22. Segel, I. H. (1993) in *Enzyme kinetics: Behavior and analysis of rapid equilibrium and steady-state enzyme systems*, Wiley, New York.
23. Roepstorff, P., and Fohlman, J. (1984) *Biomed. Mass Spectrom. 11*, 601.
24. L′abbé, G. (1990) *Bull. Soc. Chim. Belg. 99*, 281−291.

BI9721389